Noise, Time-Constant, and Hall Studies on Lead Sulfide Photoconductive Films

FRANCES L. LUMMIS AND RICHARD L. PETRITZ
United States Naval Ordnance Laboratory, White Oak, Maryland
(Received October 4, 1956)

Measurements of the noise in seven lead sulfide photoconductive films over the frequency range 20–16 000 cps show that the noise consists mainly of a $1/f$ component at frequencies below 100 cps, a generation-recombination component between 100 and 10 000 cps and a Nyquist component at higher frequencies. The data are analyzed to give the magnitude, N_{s0}(G-R), and the time constant, τ_n, of the generation-recombination noise. The signal time constant, τ_s, is found by measuring the frequency dependence of the photoconductive response. The product of the majority carrier density and the film thickness, pd, is found from measurement of the Hall voltage. Representative values are N_{s0}(G-R)$=4.5\times10^{-9}$ rms noise volts/[(dc bias volt$\times(\Delta f)^{\frac{1}{2}}$], $\tau_n=230$ μsec, $\tau_s=280$ microseconds, and $pd=3.0\times10^{12}$/cm^2.

From τ_s and pd, a theoretical value of N_{s0}(G-R) is calculated and found to be in good agreement with the experimental value. From this and the reasonable agreement between τ_s and τ_n it is concluded that these measurements furnish a verification of the theory of photoconductivity in semiconductor films recently published by one of us. Calculation shows that the generation-recombination noise is mainly due to lattice processes; less than 1% is due to radiation fluctuations. It is also shown that noise can be used in place of Hall measurements to evaluate certain semiconductor parameters.

I. INTRODUCTION

A THEORY of photoconductivity in semiconductor films of the lead salt family was recently developed[1] which considers the primary photoeffect to be a change in the number of majority carriers in the crystallites. Secondary amplification can occur from the lowering of intercrystalline barrier potentials. It was shown that the noise in such a detector should have four components: $1/f$, generation-recombination, Nyquist, and shot noise. The intercrystalline barriers give rise to a Nyquist and a shot component of noise while the crystallites give rise to a Nyquist and a generation-recombination component. The $1/f$ component is believed to be associated with surfaces and intercrystalline barriers. The Nyquist terms are independent of current, the shot term is proportional to current, and the generation-recombination and $1/f$ terms are proportional to the square of the current. For biasing currents normally used in photoconductors, the $1/f$ component dominates at low frequencies, and the Nyquist and shot components at high frequencies. Generation-recombination noise, which establishes the fundamental limit of sensitivity, should be observable in sensitive detectors at intermediate frequencies.

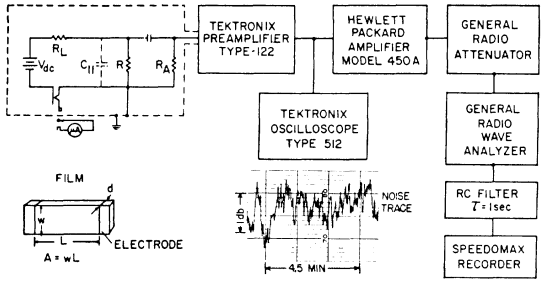

FIG. 1. Block diagram of the apparatus for noise measurements including a schematic diagram of the cell biasing circuit; sketch defining dimensions of a photoconductive film deposited on glass; and a sample recorder trace of noise voltage.

The primary generation-recombination noise is a fluctuation in the number of charge carriers (holes) in the crystallites; it will be amplified if barrier modulation occurs. The number of holes fluctuates because of fluctuations in the rate of absorption and emission of background radiation, and because of fluctuations in the rate of absorption and emission of lattice phonons. The generation-recombination noise spectrum is of the form $1/[1+(\omega\tau_s)^2]$, where τ_s is the photoconductive time constant. This spectrum is the same as the frequency dependence of the signal response to pulsed radiation.[2]

Prior to 1951, semiconductors showed[3] a noise spectrum having an inverse frequency dependence, called a $1/f$ spectrum. We began noise experiments at that time with the hope of finding a generation-recombination component in the spectrum. The chemically deposited lead sulfide film of Eastman Kodak was chosen for study because it was known to be a very sensitive detector. Photoconductive measurements[4] showed $\tau_s\cong280$ microseconds. Noise measurements[4] made over the audio-frequency range (20–16 000 cps) showed a clear deviation from the $1/f$ law which was identified as generation-recombination noise. The time constant obtained from the noise data was in reasonably good agreement with that of the signal response. This was the first experimental verification of the predicted relation[2] between the frequency dependence of the photoconductive response and the spectrum of the noise. It was also one of the first observations of a generation-recombination component of noise in semiconductors. Herzog and van der Ziel observed such a

[1] R. L. Petritz, Phys. Rev. **104**, 1508 (1956) (called I in text).

[2] R. L. Petritz, Phys. Rev. **86**, 660(A) (1952).

[3] Extensive references to papers on noise in semiconductors will be found in A. van der Ziel, *Noise* (Prentice-Hall, Inc., New York, 1955); A. van der Ziel in *Advances in Electronics* (Academic Press, Inc., New York, 1952), Vol. 4; and R. L. Petritz, Proc. Inst. Radio Engrs. **40**, 1440 (1952). Reference to papers on noise in the lead salt photoconductors will be found in T. S. Moss, Proc. Inst. Radio. Engrs. **43**, 1869 (1955).

[4] F. L. Lummis and R. L. Petritz, Phys. Rev. **86**, 660(A) (1952).

spectrum in germanium filaments at about the same time.[5]

Having observed a generation-recombination component in the noise, it then became possible to check the magnitude with predictions of the theory developed in I. To make the comparison one needs independent measurements of time constant and Hall voltage, along with noise measurements. In this paper we report such measurements and compare theory with experiment.

II. NOISE MEASUREMENTS

A. Apparatus

A block diagram of the apparatus for making the noise measurements is shown in Fig. 1. The cell, of resistance R, is biased with the voltage, V_{dc}, in series with the load resistor, R_L. The input resistance of the amplifier is $R_A=1$ megohm. For noise measurements $R_L \cong R$. The General Radio wave analyzer was used both as a variable-frequency filter and as a detector. An R-C filter with a time constant of 1 second was used to smooth the fluctuations before recording the noise

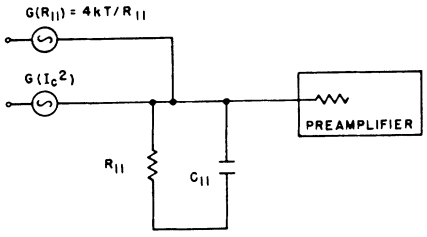

FIG. 2. Equivalent ac circuit for noise analysis given in Sec. IIB.

voltage. The noise voltage at each frequency was recorded for about five minutes; a typical recorder trace is included in Fig. 1. As evident from the trace, readings accurate to within $\frac{1}{2}$ db were easily obtained. The attenuator made it possible to keep the recorder deflection near its most sensitive position, thus minimizing calibration errors.

B. Measurement Procedure and Data Analysis

To compare experiment and theory we need to separate the G-R (generation-recombination) component of noise from Nyquist, shot and $1/f$ noise. The excess cell noise is represented by an equivalent short-circuit noise current generator $G(I_c^2)$ as shown in Fig. 2. This generator includes the $1/f$, G-R, and shot components of the cell noise. The Nyquist noise of the cell is grouped with that of the load and amplifier resistors and is represented by $G(R_{II})$ in Fig. 2. For the circuit of Fig. 1 and Fig. 2, with $V_{dc}=0$, the mean-square noise voltage in a band width Δf at the grid of

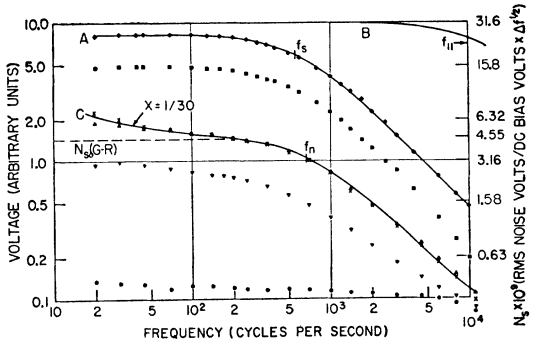

FIG. 3. Noise and signal data for cell A7-4: solid circles indicate Nyquist noise data, triangles indicate noise voltage with matched load (erect triangles for $I_{dc}=46\,\mu a$, inverted triangles for $I_{dc}=23\,\mu a$), ×'s indicate corrected noise voltage data for $I_{dc}=46\,\mu a$. All of the noise voltage curves are plotted on the same relative scale. The noise data, when read on the right-hand ordinate, is discussed in Sec. IIC. Diamonds indicate signal voltage for $R_L=50\,000$ ohms, and squares indicate signal voltage for matched load; no relation is implied for the magnitude of the signal from one curve to another.

the preamplifier is

$$\langle e^2\rangle = G(R_{II})\,|Z_{II}|^2\Delta f, \tag{1}$$

$$G(R_{II})=4kT/R_{II}, \quad G(I_c^2)=0, \tag{2}$$

$$|Z_{II}|^2=\frac{R_{II}^2}{1+(\omega\tau_{II})^2}, \quad \tau_{II}=R_{II}C_{II}, \qquad \frac{1}{R_{II}}=\frac{1}{R}+\frac{1}{R_L}+\frac{1}{R_A}. \tag{3}$$

C_{II} is the total shunt capacitance of the input circuit.

The detector in the General Radio wave analyzer is a linear detector. Theory shows[6] that the average output voltage, as taken from the recorder, is related to the spectrum of the input noise by

$$\langle V(R_{II})\rangle=[(4kT/R_{II})\,|Z_{II}(f)|^2\times\tfrac{1}{2}\pi\,|K(f)|^2\Delta f]^{\frac{1}{2}}, \tag{4}$$

where $K(f)$ is the gain of the amplifier-attenuator-filter system at the tuning frequency, f, and Δf is the band width of the filter ($\Delta f=5$ cps). Except at very low frequencies, $|K(f)^2|\Delta f$ is independent of f. Therefore the plot of $\langle V(R_{II})\rangle$ can be expected to show a drop at high frequencies where $|Z_{II}(f)|^2$ decreases. The solid circle data points of Figs. 3 and 4 are the Nyquist noise voltage for two representative cells and show this behavior.

When a dc voltage is applied across the cell and load resistor, the excess cell noise is no longer zero. The average recorder voltage is now

$$\langle V(R_{II},I_c)\rangle=\{[G(I_c^2)+4kT/R_{II}]\,|Z_{II}(f)|^2\times\tfrac{1}{2}\pi\,|K(f)|^2\Delta f\}^{\frac{1}{2}}. \tag{5}$$

[5] G. B. Herzog and A. van der Ziel, Phys. Rev. 84, 1249 (1951).

[6] J. L. Lawson and G. E. Uhlenbeck, *Threshold Signals* (McGraw-Hill Book Company, Inc., New York, 1950), Chap. 3.

The triangular points of Figs. 3 and 4 are plots of $\langle V(R_{II},I_c)\rangle$.

We find $\langle V(I_c)\rangle$, the spectral shape of $G(I_c^2)$, by solving Eqs. (4) and (5);

$$\langle V(I_c)\rangle=[G(I_c^2)\tfrac{1}{2}\pi|K(f)|^2\Delta f]^{\frac{1}{2}}R_{II}$$
$$=\{[\langle V(R_{II},I_c)\rangle^2-\langle V(R_{II})\rangle^2][1+(\omega\tau_{II})^2]\}^{\frac{1}{2}}. \quad (6)$$

That is, first the square root of the difference in the squares of the total noise data (erect triangles) and the Nyquist data (solid circles) is calculated. Then curve B, which is a plot of $[1+(\omega\tau_{II})^2]^{-\frac{1}{2}}$ is used to make the frequency correction in Eq. (6). The method of obtaining curve B will be described in Sec. IIIC. Finally, there is a small correction at low frequencies because $K(f)$ decreases in the amplifiers. The crosses (✕'s) are the data after being corrected.

The magnitude of the gain²-band-width factor, $\frac{1}{2}\pi|K(f)|^2\Delta f$, is found by calibration with the Nyquist noise. From Eq. (4) we have, at low frequencies,

$$\tfrac{1}{2}\pi|K|^2\Delta f=\langle V(R_{II})\rangle^2/4kTR_{II}. \quad (7)$$

Substituting Eq. (7) into Eq. (6) we have for the absolute magnitude of the spectrum,

$$G(I_c^2)=\frac{[\langle V(R_{II},I_c)\rangle^2-\langle V(R_{II})\rangle^2]4kT}{\langle V(R_{II})\rangle^2R_{II}}$$
$$\cong\frac{\langle V(R_{II},I_c)\rangle^2}{\langle V(R_{II})\rangle^2}\frac{4kT}{R_{II}}, \quad (8)$$
$$\omega\ll 1/\tau_{II}.$$

(C) Dependence of $G(I_c^2)$ on Biasing Current

As shown in I [Eqs. (59) and (60)], $G(I_c^2)$ should be of the form

$$G(I_c^2)=N_s^2(16I_{dc}^2/A)+2qI_{dc}/nL, \quad (9)$$

where N_s is independent of current and represents the G-R and $1/f$ components of noise, A is the cell area, $2qI_{dc}/nL$ is the shot noise of the barriers, n is the number of barriers in series per unit length of film, and L is the length of the film.

The dependence of $G(I_c^2)$ on I_{dc} was explored. The inverted triangles of Fig. 3 are data for $I_{dc}=23$ μa, while the erect triangles are for $I_{dc}=46$ μa. Examination shows $G(I_c^2)\propto I_{dc}^2$, from which we conclude that there is no shot component of noise in the region of bias current used in this study.

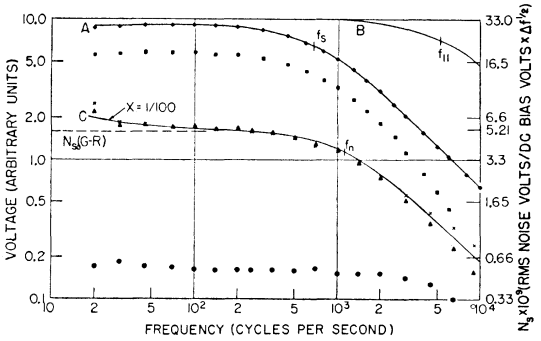

FIG. 4. Signal and noise data for cell A15-4, $I=22.4$ μa. Symbols the same as in Fig. 3.

N_s normalizes $G(I_c^2)$ to unit biasing current and unit sensitive area and is called the specific noise. We calculate N_s from our data; this is a numerical operation on the corrected data (✕'s) of Figs. 3 and 4 and does not change the frequency dependence. The right-hand ordinates of the figures are in terms of N_s.

D. Discussion

The above corrections do not change the original data appreciably at low and intermediate frequencies. However, at frequencies above 1000 cps the corrections are needed to get an accurate slope for the spectrum. The net corrections depend on the load resistor; a small value makes the capacitance correction small but increases the Nyquist noise relative to the excess cell noise as shown by Eq. (5). It was found that the matched condition, $R_L=R$, was a good compromise. Note that at high frequencies the net correction is to raise the data in Fig. 4 while in Fig. 3 it is to lower the data.

By the above analysis we have separated the excess cell noise, $G(I_c^2)$, from the Nyquist noise of the cell and load resistors; that is, we have obtained the correct frequency dependence of $G(I_c^2)$ and its absolute magnitude. Our next step in the noise analysis is to separate $G(I_c^2)$ into its G-R and $1/f$ components, but before doing this we discuss the measurement of the photoconductive time constant.

III. PHOTOCONDUCTIVE RESPONSE MEASUREMENTS

A. Apparatus

The radiation signal source was a neon bulb pulsed by a square wave generator. The cell was biased in the same manner as for the noise measurements as shown in Fig. 1, except that $R_L=50\,000$ ohms to minimize the effect of circuit capacitance. The same basic amplification setup was used, but since less gain was needed the Hewlett-Packard amplifier and the attenuator could be eliminated. Signal voltage was read directly on the wave analyzer, so the filter and recorder were not used.

B. Procedure for Measuring τ_s

The neon bulb was pulsed at frequencies ranging from 20 to 16 000 cps, and the corresponding signal voltage was read from the wave analyzer tuned to the fundamental frequency of the pulse. The diamond symbols on Figs. 3 and 4 show the signal voltage *versus* frequency. The data are fitted by curve A according to the equation,

$$V_s=V_{s0}/[1+(f/f_s)^2]^{\frac{1}{2}}, \quad \tau_s=1/2\pi f_s. \quad (10)$$

The characteristic frequency f_s is marked on each curve; we calculate τ_s and include it in Table I.

TABLE I. Cell parameters, noise, time constant, and Hall data on seven lead sulfide photoconductive films.[a] Noise values on first line; Hall values on second line.

Cell	L mm	w mm	R megohms	$\rho/d = Rw/L$ megohms	I_{dc} μa	X	N_{s0}(G-R) $\times 10^9$ rms noise volts / dc bias volts $\times(\Delta f)^{\frac{1}{2}}$	$N_s(f=90)$ $\times 10^9$	τ_n μsec	τ_s μsec	V_H mv	R_H/d $\times 10^{-6}$ cm²/coul	pd $\times 10^{-12}$ No./cm²	μ^* cm²/v-sec	N_{sr}^2(G-R)/N_s^2(G-R)	N_{si}^2(G-R)/N_s^2(G-R)
B1–4	4.1	1.0	1.2	0.30	41	1/30	3.75	4.0	250	300			4.7	4.4	0.006	0.994
		0.74	2.15	0.39	3.75		5.1				0.45	2.6	2.9	5.6		
B2–2	4.1	1.0	1.8	0.45	32	1/100	6.15	6.15	290	400			2.6	3.4	0.007	0.993
		0.58	5.0	0.72	2.05		6.95				0.34	3.55	2.1	4.2		
B2–3	4.1	1.0	1.6	0.40	18	1/30	3.8	4.3	170	260			4.5	3.4	0.015	0.985
		0.64	2.9	0.45	3.2		6.6				0.73	4.9	1.5	9.1		
C2–2D	3.2	0.5	3.0	0.47	16	1/30	3.6	4.6	93	215			4.2	3.15	0.004	0.996
		0.36	3.95	0.44	2.5		4.5				0.33	2.8	2.6	5.4		
A7–4	3.0	2.5	0.52	0.43	46	1/30	4.55	5.1	230	280			3.4	4.25	0.004	0.996
		1.75	0.57	0.33	7.8		4.8				0.91	2.45	3.0	6.3		
A15–4	3.0	2.5	1.1	0.92	22	1/100	5.2	5.5	140	230			2.1	3.2	0.001	0.999
		2.5	1.3	0.92	5.5		4.1				0.28	2.1	3.5	2.0		
15–2	3.0	3.0	0.415	0.415	135	1/30	3.4	4.0	215	265			5.6	2.7	0.005	0.995
		3.0	0.30	0.30	21		4.7				0.98	2.5	3.0	5.0		

[a] $H = 9.4 \times 10^3$ gauss except for cell 15-2 where $H = 3.7 \times 10^3$ gauss.

C. Determination of Circuit Capacitance Correction

As mentioned in Sec. IIB, it was necessary to use a load resistance approximately equal to the cell resistance for the noise measurements. Our method of determining the frequency correction of the $R_{II}C_{II}$ effect was to make a second signal run with R_L equal to the value used in the noise run. These data are plotted in Figs. 3 and 4 using square symbols. Curve B illustrates the difference in frequency dependence of the two signal curves (diamonds and squares) and gives directly a plot of $[1+(\omega\tau_{II})^2]^{-\frac{1}{2}}$, which was used in Eq. (6).

IV. ANALYSIS OF EXCESS NOISE INTO GENERATION-RECOMBINATION AND 1/f COMPONENTS

From Eq. (60) of I, we write

$$N_s^2 = N_{s0}^2(\text{G-R})/[1+(f/f_n)^2] + N_{s0}^2(1/f)/(f/f_n),$$
$$N_s = N_{s0}(\text{G-R})\{[1/1+(f/f_n)^2] + X/(f/f_n)\}^{\frac{1}{2}}, \quad (11)$$

where

$$f_n = 1/2\pi\tau_n, \quad X = N_{s0}(1/f)/N_{s0}(\text{G-R}),$$

and the subscript 0 indicates frequency independence of the coefficients.

From the theory of I, f_n should be equal to f_s, but we did not assume this to be the case in the following analysis. To find N_{s0}(G-R), X, and f_n from the corrected data (✕'s) of Figs. 3 and 4, the family of curves shown in Fig. 5 were calculated from Eq. (11). An overlay was drawn from which the best fit was obtained; curves C of Figs. 3 and 4 were obtained in this way. X, f_n and N_{s0}(G-R) are shown on the figures and are listed in Table I; $N_s(f=90)$ is also tabulated.

In Fig. 3, curve C fits the data over the whole frequency range, while in Fig. 4 the curve deviates from the data at high frequencies. In fitting the data, preference was given to the knee of the curve since this is the region where the G-R term is most pronounced.

Table I lists the significant parameters of seven different cells. The amount of $1/f$ noise present relative to G-R noise is shown by the value of X; $X=1/100$ indicates very little $1/f$ noise. Noisy cells in which $X>1/30$ are not included.

While theory indicates that f_n should equal f_s, it was found that the best fit could not be obtained with this assumption; rather it was obtained with f_n 20–30% greater than f_s as is shown on the figures and in the table. This is discussed further in Sec. VI.

V. HALL VOLTAGE MEASUREMENTS

A. Apparatus

The experimental apparatus is a modification of that described by Woods[7] and is shown in Fig. 6. The 4-μf

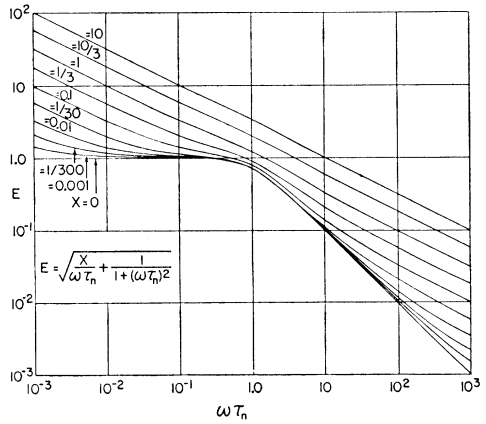

FIG. 5. Theoretical curves for determining the ratio, X, of $1/f$ to generation-recombination noise, as given by Eq. (11).

[7] J. F. Woods in *Photoconductivity Conference*, edited by Breckenridge, Russell, and Hahn (John Wiley and Sons, Inc., New York,

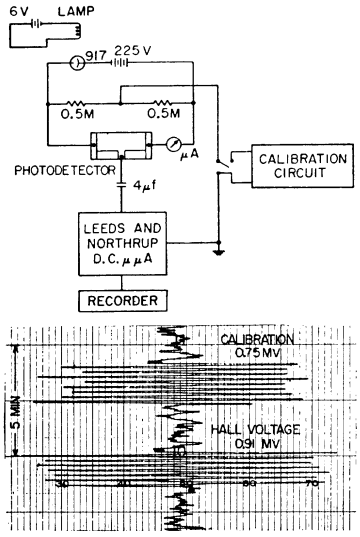

FIG. 6. Block diagram of apparatus for Hall measurements; constant current source shown in top of diagram; and sample recorder traces of Hall and calibration voltage.

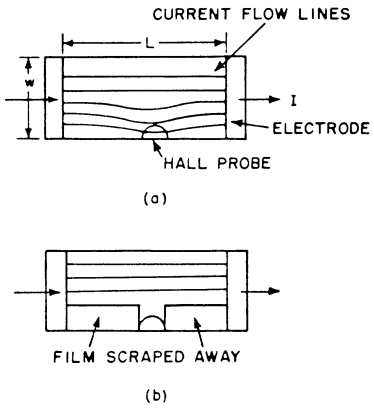

FIG. 7. Illustration of current flow lines in a thin film; (a) Hall probe extending into film, and (b) film scraped away from sides of Hall probe.

condenser is used to filter out dc and very-low-frequency drift. The magnetic field is reversed at a frequency of 1/14 cps. Provision is made to insert a calibrating voltage in series with the Hall circuit.

An improvement of Woods' system was the use of the constant current supply shown in Fig. 6. The photocell has a nearly infinite impedance whose current can be controlled by the light intensity. Thus drift in the Hall voltage due to changes in cell resistance is reduced because the current is held constant by the phototube.

B. Procedure

Measurements of the Hall coefficient were made on the same cells used in the noise studies. Hall contacts made by painting a small Aquadag electrode on the cell as shown in Fig. 7(a) proved to be very noisy. A Hall voltage reading was possible on only two of the seven films. Montgomery[8] has pointed out that such a contact could be quite noisy even though no current flows out of the contact. This is because current flows through the contact as shown in Fig. 7(a). The configuration shown in Fig. 7(b) minimizes such contact noise as first shown by Montgomery. The films were therefore scraped to this shape and the noise was considerably reduced. Easily measurable Hall voltages were then obtained on all the films. Figure 6 includes a typical recorder trace of the Hall and calibration voltages; the Hall voltage, V_H, is given in Table I.

We calculate

$$R_H/d=2V_H\times10^8/HI_{\rm dc}\ \text{cm}^2/\text{coulomb}, \qquad (12)$$

where H is the magnetic field, $I_{\rm dc}$ is the total current through the cell, and d is the thickness of the film. The factor two is necessary because of the one probe configuration. We did not attempt to measure d since it is combined with R_H in the theoretical expressions.

VI. INTERPRETATION

We now compare our data with the predictions of the theory developed in I. There we find as an expression for the specific G-R noise,

$$N_s(\text{G-R})=N_{s0}(\text{G-R})/[1+(\omega\tau_s)^2]^{\frac{1}{2}},$$
$$N_{s0}(G\text{-}R)=(1+B)\times\tfrac{1}{2}(\tau_s/pd)^{\frac{1}{2}}. \qquad (13)$$

A normalized expression for the signal response, called the specific responsivity, is

$$R_s=\frac{(1+B)\eta_s\tau_s}{4pdh\nu_s[1+(\omega\tau_s)^2]^{\frac{1}{2}}}. \qquad (14)$$

B represents barrier modulation effects; if no barrier modulation occurs, $B=0$, while for large barrier modulation $B\gg1$. η_s is the quantum efficiency at the spectral frequency, ν_s, of the signal radiation, h is Planck's constant, and p is the density of majority carriers in the crystallites.

A. Comparison of Time Constants Obtained from Signal and Noise Measurements

Comparison of Eq. (13) with Eq. (14) shows that the G-R noise should have the same frequency dependence as the signal response. Comparison of curve A of Fig. 3 with curve C shows the similarity between the signal and noise curves. A more precise comparison is made by comparing τ_n, the time constant found from the noise analysis, with τ_s, the time constant of the signal response. These quantities are listed in Table I and are seen to be in qualitative agreement. However, τ_n is consistently 20–30% less than τ_s. This discrepancy may arise because the best fit of the curves of Fig. 5 to the data depends on the shape of the noise spectrum in the high-frequency range. As discussed in Sec. IIB, this range must be corrected for both circuit capacitance and Nyquist noise. It is therefore possible that we

1956), p. 636; Phys. Rev. **99**, 658(A) (1955); and thesis, The Catholic University of America, Washington, D. C., 1956 (to be published).

[8] H. C. Montgomery, Bell System Tech. J. **31**, 950 (1952).

cannot expect better than 20% accuracy in our value for τ_n. However, since τ_n is consistently less than τ_s the difference appears to be real, indicating that the theory may need extension. For example, the noise associated with minority carriers has been neglected in the model.

B. Comparison of the Theoretical and Experimental Magnitude of Noise

A second comparison of theory and experiment can be made in the magnitude of the noise. Equation (13) shows that we need independent measurements of pd, τ_s and B to predict a theoretical value of N_{s0}(G-R). We obtain pd from our Hall measurements,

$$pd=3\pi d/8qR_H, \tag{15}$$

where R_H/d was found by Eq. (12); pd is given in Table I (second line of data for each film). τ_s was measured by signal response as described in Sec. IIIB. Woods has found B to be zero in this type of film by measuring the change in Hall coefficients and resistivity under illumination.[7]

Using $B=0$ and our values for pd and τ_s, we use Eq. (13) to calculate a theoretical value of N_{s0}(G-R) for each film. This is also listed in the second line of data for each film. The corresponding experimental value of N_{s0}(G-R), as found directly by noise measurements, is given on the first line. Inspection shows generally good agreement between the two values. We do not expect exact agreement because the noise and Hall data were taken at different times and the characteristics of these cells change somewhat from day to day. Furthermore, the cells had to be scraped to obtain satisfactory Hall measurements as mentioned above. This scraping was done after the noise measurements had been completed. In the table we list the resistance per unit area,

$$\rho/d=Rw/L, \tag{16}$$

when the noise data were taken (first lines) and when Hall measurements were made (second lines). It is seen that while no radical change resulted from scraping and aging, some changes had occurred.

C. Conclusion

In summary, the general agreement between N_{s0}(G-R, theory) and N_{s0}(G-R, expt) and between τ_n and τ_s constitutes a verification of the theory of photoconductivity developed in I. Further investigation is required to explain the 20–30% difference between τ_n and τ_s.

VII. IS THE PbS DETECTOR SEEING RADIATION NOISE?

In I we show that the G-R noise arises from fluctuations in radiative and lattice processes. The noise expression which explicitly shows these two sources is Eq. (53) of I:

$$N_s(\text{G-R})=\frac{(1+B)\tau_s(\eta_r J_r+\eta_l J_l)^{\frac{1}{2}}}{2pd[1+(\omega\tau_s)^2]^{\frac{1}{2}}}. \tag{17}$$

$\eta_r J_r$ and $\eta_l J_l$ are respectively the mean background radiation flux in photons/cm² sec and the mean flux of the lattice vibrations in phonons/cm² sec absorbed by the electronic system of the detector. Formal expressions for $\eta_r J_r$ and $\eta_l J_l$ are given by Eqs. (37) to (42) of I.

In order to determine whether these PbS cells are limited by radiation noise, we set $J_l=0$ and calculate

$$N_{sr}(\text{G-R})=N_s(\text{G-R}, J_l=0). \tag{18}$$

An exact expression for $\eta_r J_r$ is

$$\eta_r J_r=\tfrac{1}{4}c\int_0^\infty \eta(\nu)n_r(\nu)d\nu \text{ quanta/cm}^2\text{ sec},$$
$$n_r(\nu)=8\pi\nu^2/c^2(e^{h\nu/kT}-1), \tag{19}$$

where $\eta(\nu)$ is the quantum efficiency at a spectral frequency ν and $n_r(\nu)$ is the density of photons in the background radiation field. The wavelength dependence of the quantum efficiency can be derived from the spectral dependence of the responsivity according to Eq. (14). The absolute value of η can be estimated from crystal absorption data as discussed in I, Sec. VI. With such data, a graphical integration of Eq. (19) can be performed. Moss has done approximately this for PbS.[9] He has graphically integrated the product of the responsivity curve and the blackbody formula, obtaining the flux in watts/cm² absorbed by the detector. He assumes $\eta\rightarrow 1$ at short wavelengths. To find the quanta/cm² sec he divides his power expression by hc/λ_r, where $\lambda_r=2.9\mu$. His result for $\eta_r J_r$ is 2.9×10^{13} quanta/cm²-sec.

A simple approximation for $\eta_r J_r$ is to use for η_r the value of the quantum efficiency in the spectral region of maximum photoresponse, and for J_r,

$$J_r=\tfrac{1}{4}c\int_{E_i/h}^\infty n_r(\nu)d\nu, \tag{20}$$

where E_i is the intrinsic energy gap of the semiconductor. J_r has been evaluated by Eq. (20), neglecting the minus one in the denominator of $n_r(\nu)$. This approximation is valid for infrared photoconductive detectors. The resulting values of J_z for some detectors of current interest are listed in Table I of Petritz's work.[10] For lead sulfide we used $E_i=0.41$ ev and found $J_r=3.5\times 10^{13}$ quanta/cm² sec. The agreement of this with Moss's value indicates that the approximation is reasonably good. We shall use his value here but mention the approximate method because it may find use when spectral data are not available, or when a rough estimate is sufficient.

[9] T. S. Moss, J. Opt. Soc. Am. **40**, 602 (1950).

[10] R. L. Petritz in *Photoconductivity Conference*, edited by Breckenridge, Russell, and Hahn (John Wiley and Sons, Inc., New York, 1956), p. 49.

We calculate N_{sr}(G-R) from Eqs. (17) and (18) using Moss's value for $\eta_r J_r$, our measured values of τ_s and pd, and $B=0$. The results are expressed as the ratio $[N_{sr}(\text{G-R})/N_s(\text{G-R})]^2$ in Table I; the experimental noise value is used for N_s(G-R).

Lacking independent information concerning $\eta_l J_l$, we cannot directly calculate the lattice contribution to the noise. However, we can calculate

$$N_{sl}^2(\text{G-R})=N_s^2(\text{G-R})-N_{sr}^2(\text{G-R}) \\ =N_s^2(\text{G-R})\{1-[N_{sr}(\text{G-R})/N_s(\text{G-R})]^2\}, \quad (21)$$

using the experimental noise value for N_s(G-R) and the calculated value of $[N_{sr}(\text{G-R})/N_s(\text{G-R})]^2$. The results are tabulated as $[N_{sl}(\text{G-R})/N_s(\text{G-R})]^2$ in Table I.

Comparison of

$$[N_{sl}(\text{G-R})/N_s(\text{G-R})]^2 \text{ with } [N_{sr}(\text{G-R})/N_s(\text{G-R})]^2$$

shows that the noise is principally due to interaction with the lattice. J_r would have to be at least 100 times larger for the observed noise to be due to radiation fluctuations. Thus, we do not agree with Wolfe's[11] conclusion that Eastman-Kodak PbS cells are limited by radiation noise at room temperature. It should be possible to decrease J_l by cooling and thereby reach the radiative limit.

VIII USE OF NOISE INSTEAD OF HALL MEASUREMENTS TO EVALUATE SEMICONDUCTOR PARAMETERS

It is not always desirable or convenient to place a Hall probe on a film. When this is the case, the G-R noise provides a method of evaluating semiconductor parameters.[2] On the basis of the above theory, we can use the noise data to calculate pd from Eq. (13). Table I (first lines) lists pd calculated this way; they are seen to be in reasonable agreement with the Hall values (second lines).

The effective mobility can be found from the defining equation,

$$\mu^*=[q(\rho/d)(pd)]^{-1}, \quad (22)$$

where we use pd as found by the noise data and ρ/d from Eq. (16). The values of μ^* thus calculated are listed in Table I (first lines) for comparison with those calculated from Hall values (second lines),

$$\mu^*=\tfrac{3}{8}\pi\mu_H, \quad (23)$$

$$\mu_H=(R_H/d)(d/\rho). \quad (24)$$

It is of interest to note that we calculated μ^* from noise data as described above at the time of our first measurements[4]; we assumed $B=0$. The values found were in reasonable agreement with values found by Lothrup,[12] who obtained μ^* on evaporated films of PbS from Hall and resistivity measurements. Thus our noise measurements and their interpretation were the first indication that no appreciable barrier modulation occurs in these films. The Hall and resistivity studies of Woods[7] were of course necessary to establish directly that $B=0$.

Another use of the noise measurements is to evaluate the quantum efficiency. Substituting Eq. (13) into Eq. (14) and solving for η_s, we obtain

$$\eta_s=R_s h\nu_s(1+B)/N_s^2(\text{G-R}). \quad (25)$$

Thus responsivity and noise measurements can be used to evaluate the quantum efficiency without Hall measurements, if we assume that B is known.

In conclusion, we emphasize that Hall measurements are preferable to noise measurements as a method of finding pd and related quantities. The noise should be considered as a supplemental method, useful when it is not desirable or convenient to place a Hall probe on the film. It is obviously necessary that the noise spectrum show the presence of G-R noise for this procedure to be valid. Unfortunately in most semiconducting films, $1/f$ noise still dominates the G-R noise.[13]

IX. CONCLUSIONS

This study has shown that the noise in chemically deposited lead sulfide films is dominated by a $1/f$ term below 100 cps, a generation-recombination component between 100 and 10 000 cps, and finally by Nyquist noise at higher frequencies. The data have been analyzed to give a magnitude and time constant for the generation-recombination component and a magnitude for the $1/f$ component. The values of time constant as found by noise measurements are in reasonably good agreement with those measured by photoconductive response, although somewhat lower. The magnitude of the noise is in general agreement with values predicted from theory. This constitutes a verification of the theory of photoconductivity in semiconductor films developed in I and outlined in the introduction of this paper. The generation-recombination noise is due mainly to interactions with the lattice; radiation noise accounts for less than 1% of the observed noise. Furthermore, noise measurements are shown to be a useful supplement to Hall measurements for evaluating semiconductor parameters when the generation-recombination noise is observable.

X. ACKNOWLEDGMENTS

The authors wish to express their appreciation to Dr. James N. Humphrey, Dr. Wayne W. Scanlon, and Dr. Joseph F. Woods for many helpful discussions of experimental problems and interpretation of results.

[11] B. Wolfe, Rev. Sci. Instr. **27**, 60 (1956).

[12] E. W. Lothrup, Jr., thesis, Northwestern University, Evanston, Illinois, 1949 (unpublished).

[13] D. Barker, Proc. Phys. Soc. (London) **B68**, 898 (1955).